Crystal Structure of Phosphatidylinositol-Specific Phospholipase C from *Bacillus cereus* in Complex with Glucosaminyl(α1→6)-D-*myo*-inositol, an Essential Fragment of GPI Anchors[†,‡]

Dirk W. Heinz,*[,§] Margret Ryan,[||,⊥] Miles P. Smith,[⊥] Larry H. Weaver,[||,▽] John F. W. Keana,[⊥] and O. Hayes Griffith*[,||,⊥]

Institut für Organische Chemie und Biochemie, Universität Freiburg, D-79104 Freiburg, Germany, and Institute of Molecular Biology, Departments of Physics and Chemistry, and Howard Hughes Medical Institute, University of Oregon, Eugene, Oregon 97403

Received March 12, 1996; Revised Manuscript Received May 16, 1996[⊗]

ABSTRACT: Numerous proteins on the external surface of the plasma membrane are anchored by glycosylated derivatives of phosphatidylinositol (GPI), rather than by hydrophobic amino acids embedded in the phospholipid bilayer. These GPI anchors are cleaved by phosphatidylinositol-specific phospholipases C (PI-PLCs) to release a water-soluble protein with an exposed glycosylinositol moiety and diacylglycerol, which remains in the membrane. We have previously determined the crystal structure of *Bacillus cereus* PI-PLC, the enzyme which is widely used to release GPI-anchored proteins from membranes, as free enzyme and also in complex with *myo*-inositol [Heinz, D. W., Ryan, M., Bullock, T. L., & Griffith, O. H. (1995) *EMBO J. 14*, 3855−3863]. Here we report the refined 2.2 Å crystal structure of this enzyme complexed with a segment of the core of all GPI anchors, glucosaminyl(α1→6)-D-*myo*-inositol [GlcN-(α1→6)Ins]. The *myo*-inositol moiety of GlcN(α1→6)Ins is well-defined and occupies essentially the same position in the active site as does free *myo*-inositol, which provides convincing evidence that the enzyme utilizes the same catalytic mechanism for cleavage of PI and GPI anchors. The *myo*-inositol moiety makes several specific hydrogen bonding interactions with active site residues. In contrast, the glucosamine moiety lies exposed to solvent at the entrance of the active site with minimal specific protein contacts. The glucosamine moiety is also less well-defined, suggesting enhanced conformational flexibility. On the basis of the positioning of GlcN(α1→6)Ins in the active site, it is predicted that the remainder of the GPI-glycan makes little or no specific interactions with *B. cereus* PI-PLC. This explains why *B. cereus* PI-PLC can cleave GPI anchors having variable glycan structures.

A growing number of membrane proteins are being identified as tethered to the membrane by a glycosylphosphatidylinositol[1] (GPI) anchor, rather than by a hydrophobic part of the protein (Turner, 1990; Takeda & Kinoshita, 1995). Rapid identification of GPI-linked proteins has been made possible because *Bacillus cereus* phosphatidylinositol-specific phospholipase C (PI-PLC), and those from *Bacillus thuringiensis*, *Staphylococcus aureus*, and *Clostridium novyi*, can release most GPI-anchored proteins from membranes. Early studies established the protein's covalent linkage to a phosphatidylinositol (PI), although the quantities of released protein were too small for extensive analysis [for a review see Low (1989)]. The discovery that the variant surface glycoprotein (VSG) from *Trypanosoma brucei* is linked to the cell surface via a GPI anchor (Ferguson et al., 1985) removed this limitation, since VSG can be obtained in large quantities for chemical and structural analysis. The structure of the GPI anchor of VSG was reported in 1988 (Ferguson et al., 1988). A range of proteins have been established to be GPI-anchored using bacterial PI-PLCs as diagnostic tools for the selective release in combination with structural analysis. These include acetylcholinesterases, 5′-nucleotidase and other cell surface hydrolases, protozoan coat proteins, activation antigens of the immune system, adhesion molecules, scrapie prion protein, and the carcinoembryonic antigen, a human tumor marker [for reviews, see Ferguson and Williams (1988), Low and Saltiel (1988), Rosenberry et al. (1989), Englund (1993), and Takeda and Kinoshita (1995)]. Because of the broad diversity of these proteins, the functional importance of their GPI anchors is not yet clear. Of significance is the increased lateral mobility of GPI anchors compared to that of hydrophobic polypeptide anchors, the regulated release by GPI cleavage, the role in cellular distribution of proteins (e.g. apical targeting of proteins in polarized cells), the exclusion from clathrin-coated pits, uptake of small molecules involving caveolae, and the possible link to signal transduction (Ferguson & Williams, 1988; Lisanti et al., 1990; Anderson et al., 1992). At least

[†] This work was supported by the Deutsche Forschungsgemeinschaft, Land Baden-Württemberg to D.W.H., NIH Grant GM 27137 to J.F.W.K., NIH Grant GM25698 to O.H.G., and NIH Grant GM 20066 to B. W. Matthews.

[‡] The X-ray coordinates have been deposited in the Brookhaven Protein Data Bank (file name 1GYM).

* Authors to whom correspondence should be addressed.

[§] Universität Freiburg.

[||] Institute of Molecular Biology, University of Oregon.

[⊥] Department of Chemistry, University of Oregon.

[▽] Department of Physics and Howard Hughes Medical Institute, University of Oregon.

[⊗] Abstract published in *Advance ACS Abstracts,* July 1, 1996.

[1] Abbreviations: DAG, 1,2-diacyl-*sn*-glycerol; GlcN(α1→6)Ins, glucosaminyl(α1→6)-D-*myo*-inositol; GPI, glycosylphosphatidylinositol; GPI-PLC, GPI-specific phospholipase C; GPI-PLD, GPI-specific phospholipase D; I(1:2cyc)P, *myo*-inositol 1:2-cyclic phosphate; Man, mannose; PI, phosphatidylinositol; PI-PLC, phosphatidylinositol-specific phospholipase C; VSG, variant surface glycoprotein.

S0006-2960(96)00610-1 CCC: $12.00

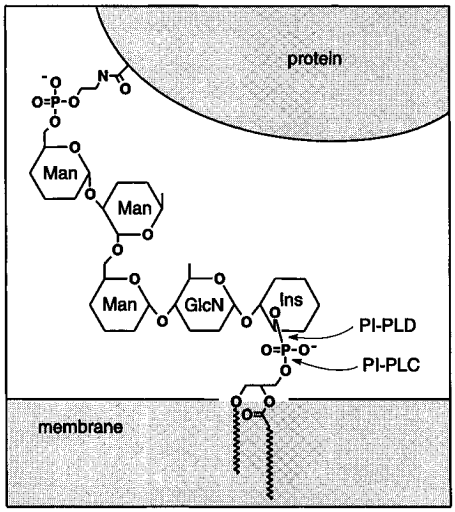

FIGURE 1: General structure of GPI anchors. The carboxy terminus of the GPI-anchored protein forms an amide bond to ethanolamine, which is linked by a phosphate to a glycan core consisting of a linear chain of three mannose rings (Man) and terminating in glucosamine (GlcN), which is bonded to the 6-OH of the *myo*-inositol ring (Ins) of PI. The lipid shown is a 1-alkyl-2-acyl glycerol. Most GPI anchors have additional branching residues in the glycan core. The point of cleavage by PI-PLCs, including *B. cereus* PI-PLC, and GPI-PLCs is marked by an arrow. For reference, the point of cleavage by (G)PI-PLDs is also shown.

one disease, paroxysmal nocturnal hemoglobinurea (PNG), is thought to be linked to a deficiency in GPI synthesis (Takeda & Kinoshita, 1995).

The structure of GPI anchors is illustrated in Figure 1. Common to *T. brucei* VSG and other GPIs is the "core structure"; the protein carboxy terminus forms an amide bond to ethanolamine-phospho-6Man(α1→2)Man(α1→6)Man-(α1→4)GlcN which in turn is glycosidically linked to the 6 hydroxyl group of PI. Variations in the structure of GPIs occur as additions to the glycan moiety, as well as differences in the lipid composition of PI. Bacterial PI-PLCs cleave the GPI anchor to release diacylglycerol (DAG) and the water-soluble portion of the GPI attached to the protein (Figure 1). In some cases, additional fatty acids are found esterified to 2-OH of *myo*-inositol, hindering cleavage by *B. cereus* PI-PLC and other bacterial PI-PLCs.

Recently, we reported the first crystal structure of a PI-PLC, the structure of *B. cereus* PI-PLC in complex with *myo*-inositol solved at 2.6 Å resolution (Figure 2). This structure provides insight into the mechanism of cleavage of PI (Heinz et al., 1995). The question we address here is how *B. cereus* PI-PLC binds to and cleaves the bulky GPI anchors. This question is relevant not only to *B. cereus* PI-PLC but also to all bacterial PI-PLCs that exhibit GPI-cleaving activity, and to the GPI-PLCs of the protozoan parasite *T. brucei* and the pathogenic fungus *Paracoccidioides brasiliensis* (Heise et al., 1995). There is also evidence for GPI-PLCs in yeast (Müller et al., 1996), the endoparasitic trematode *Fasciola hepatica* (Hawn & Strand, 1993), and mammalian cells (Vogel et al., 1992; Han et al., 1994). As a first step toward understanding the detailed molecular interactions between GPI and PI-PLC, a fragment of the GPI core structure adjacent to the cleavage point, GlcN(α1→6)Ins (Figure 3), was synthesized and cocrystallized with *B. cereus* PI-PLC. Here we report the crystal structure of this complex at 2.2 Å resolution.

EXPERIMENTAL PROCEDURES

Synthesis of 6-O-(2′-Amino-2′-deoxy-α-D-glucopyranosyl)-D-myo-inositol [GlcN(α1→6)Ins] (Figure 3). The synthesis of GlcN(α1→6)Ins via the enzymatic cleavage of the corresponding 1-phosphate has been previously reported (Plourde et al., 1992). The minute quantities of GlcN-(α1→6)Ins obtained, however, precluded full spectral characterization. For the present study, sufficient quantities of GlcN(α1→6)Ins were required for crystallographic as well as spectral characterization, which necessitated the use of a modified route. GlcN(α1→6)Ins was readily prepared directly from the selectively protected compound 6-*O*-(2′-azido-3′,4′,5′-tri-*O*-benzyl-2′-deoxy-α-D-glucopyranosyl)-2,3:4,5-di-*O*-cyclohexylidenyl-D-*myo*-inositol (Plourde et al., 1992). A suspension of this compound (50 mg, 0.063 mmol) and 20% $Pd(OH)_2$/C in MeOH (10 mL) was shaken on a Parr hydrogenation apparatus for 18 h under H_2 (50 psi). The resulting suspension was filtered through a plug of Celite, and the solids obtained were washed with MeOH (3 × 5 mL). The combined solvents were concentrated *in vacuo*, and the crude residue obtained was stirred in AcOH/

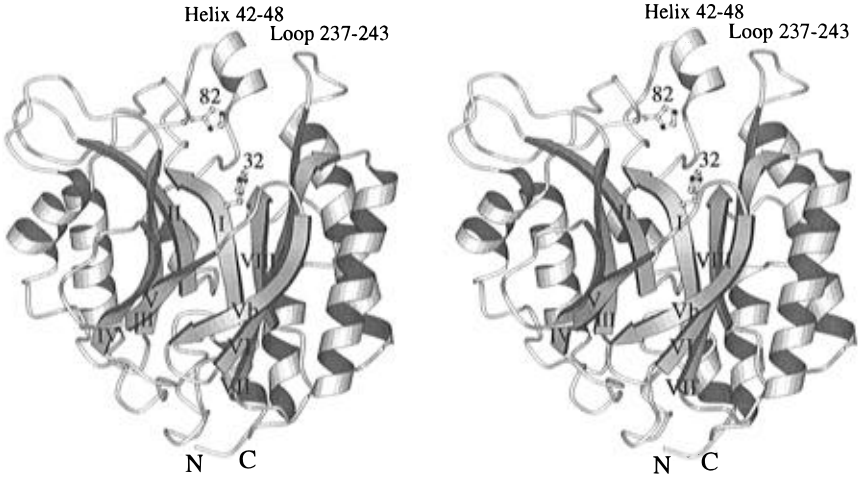

FIGURE 2: Structure of *B. cereus* PI-PLC (Heinz et al., 1995) viewed nearly perpendicular to the central β-barrel axis. Stereo ribbon representation where α-helices are shown as spirals and β-strands as arrows. The active site pocket is located at the C-terminal end of the β-barrel. The β-strands are marked by Roman numbers. The side chains of His32 and His82 are shown and labeled. The back of the active site pocket is closed by the helix comprising residues 42−48 and the loop comprising residues 237−243 (see text). This plot as well as Figures 6−8 were generated using MOLSCRIPT (Kraulis, 1991).

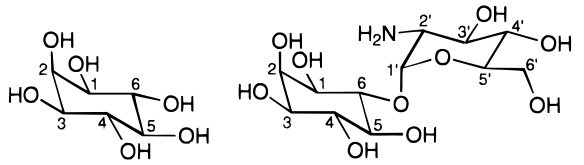

myo-inositol GlcN(α1→6)Ins

FIGURE 3: Two molecules that have been successfully cocrystallized with *B. cereus* PI-PLC: (left) *myo*-inositol, the molecule used to identify the active site of the enzyme (Heinz et al., 1995); and (right) glucosaminyl(α1→6)-D-*myo*-inositol, abbreviated GlcN(α1→6)Ins, cocrystallized with *B. cereus* PI-PLC for the present study.

water (2.5 mL, 1:1) for 3 h. The solvents were removed *in vacuo*, and the crude residue was washed with $CHCl_3$ (1 mL) and disolved in water (1 mL). Precipitation with acetone afforded GlcN(α1→6)Ins (14.5 mg, 67%) as a white solid: ^{1}H NMR (500 MHz, D_2O) δ 5.47 (d, 1 H, H1′, $J_{1'2'}$ = 3.5 Hz), 4.09 (br d, 1 H, H5′), 4.08 (ψt, 1 H, H2, $J_{21} \approx J_{23} = 2.2$ Hz), 3.94 (dd, 1 H, H3′, $J_{3'2'} = 10.7$ Hz, $J_{3'4'} = 9.2$ Hz), 3.88−3.87 (m, 2 H, H6′), 3.79 (m, 2 H, H3 and H4), 3.70 (ψt, 1 H, H6, $J_{61} \approx J_{65} = 9.6$ Hz), 3.59 (ψt, 1 H, H4′, $J_{4'3'} \approx J_{4'5'}$), 3.56 (dd, 1 H, H1), 3.44 (br t, 1 H, H5), 3.33 (dd, 1 H, H2′); ^{13}C NMR (75 MHz, D_2O) δ 97.1, 80.8, 73.0, 72.9, 72.7, 72.5, 72.0, 71.3, 70.6, 69.7, 60.5, 54.9.

Crystallization. PI-PLC from *B. cereus* was overexpressed and purified from *Escherichia coli* as described before (Koke et al., 1991; Molecular Probes Inc., Eugene, OR). Crystallization of the complex between *B. cereus* PI-PLC and GlcN(α1→6)Ins was performed by hanging drop vapor diffusion at 4 °C using similar crystallization conditions as described (Bullock et al., 1993). Droplets were prepared by mixing 4 μL of the premixed complex [8 mg/mL PI-PLC, 30 mM GlcN(α1→6)Ins, 20 mM HEPES (pH 7), and 0.01% NaN_3] and 4 μL of precipitant solution [37% PEG 600, 0.19 M trisodium citrate, 20 mM HEPES (pH 7), and 2.5 mM β-mercaptoethanol]. The drop was placed over a reservoir containing 1 mL of 2.25 M NaCl. Crystals suitable in size for data collection were obtained after 5−6 weeks. For mounting of the crystal, the drop was diluted using 30 mM GlcN(α1→6)Ins in 80% precipitant solution.

Data Collection and Structure Determination. X-ray data to 2.2 Å resolution were collected on a Xoung-Hamlin area detector (Hamlin, 1985) using graphite-monochromated CuKα radiation from a Rigaku RU-200BH rotating anode X-ray generator operated at 6 kW. Data were subsequently processed using the supplied detector software (Howard et al., 1985). The data collection statistics are summarized in Table 1. An initial $F_o - F_c$ electron density map was computed using all reflections from 10 to 2.2 Å resolution and the 2.6 Å model of uncomplexed PI-PLC including all solvent molecules (Heinz et al., 1995) for phasing. At that stage, the PI-PLC structure (without solvent molecules) was subjected to rigid body and reciprocal space least squares refinement against the new data using the program X-PLOR 3.1 (Brünger et al., 1989) employing force-field parameters by Engh and Huber (1991), in order to minimize differences between the new structure and the model structure due to slight nonisomorphism and to raise the signal corresponding to the GlcN(α1→6)Ins molecule. The coordinates for GlcN(α1→6)Ins were generated and energy-minimized using the program SYBYL 6.1 (Tripos Inc., St. Louis). Subsequently, the GlcN(α1→6)Ins molecule was positioned in the active site of PI-PLC using a newly calculated $F_o - F_c$ electron density map. The model was subjected to several cycles of slow-cooling simulated annealing, positional and restrained *B*-factor refinement, as well as manual corrections using the program O 5.9 (Jones et al., 1991). Solvent molecules were gradually incorporated into the structure using an automatic water-fitting procedure (program AWAT; Meyer, 1996). Progress in refinement was monitored by closely watching the decrease of R_{free} (Brünger, 1992). The quality of the final model was assessed using the programs PROCHECK (Morris et al., 1992) and WHATCHECK (Vriend & Sander, 1993).

Table 1: Crystallographic Data Collection and Refinement Statistics

	Data Collection
space group	$P2_12_12_1$
cell dimensions	
a, *b*, *c* (Å)	45.2, 46.5, 161.0
α, β, γ (deg)	90, 90, 90
measured reflections	32130
unique reflections	15359
maximum resolution (Å)	2.2
average I/σ_I	
overall	11.3
(2.22−2.20 Å)	3.1
data completeness (%)	
(8−2.2 Å)	75.0
(2.5−2.2 Å)	62.2
R_{sym} (%)[a] (all data)	4.74
	Refinement
resolution range (Å)	8−2.2
number of reflections ($F > 1\sigma$)	14670
number of protein atoms	2991
number of solvent atoms	137
number of GlcN(α1→6)Ins atoms	23
R-factor (%)[b]	17.8
R_{free} (%)[c]	27.2
$\Delta_{\text{bond lengths}}$ (Å)[d]	0.015
$\Delta_{\text{bond angles}}$ (deg)[d]	1.8
$\Delta_{\text{torsion angles}}$ (deg)[d]	24.8
$\Delta_{\text{improper angles}}$ (deg)[d]	1.8
average *B*-values (Å^2)	
protein atoms	20.5
solvent atoms	30.1
GlcN(α1→6)Ins atoms	31.3

[a] $R_{sym} = \sum_{hkl}\sum_i |I_{(hkl,i)} - \langle I_{(hkl)}\rangle| / \sum_{hkl}\sum_i \langle I_{(hkl)}\rangle$, where $I_{(hkl,i)}$ is the scaled intensity of the ith measurement and $\langle I_{(hkl)}\rangle$ is the mean intensity for that reflection. [b] *R*-factor $= \sum||F_o| - |F_c||\sum|F_o|$, where $|F_o|$ and $|F_c|$ are the observed and calculated structure factor amplitudes, respectively. [c] 10% of reflections omitted (Brünger, 1992). [d] $\Delta_{\text{bond lengths}}$, $\Delta_{\text{bond angles}}$, $\Delta_{\text{torsion angles}}$, and $\Delta_{\text{improper angles}}$ give the average discrepancy between these parameters in the refined structure and their "ideal" values.

RESULTS

Structure Determination and Quality of the Model. The crystal structure of PI-PLC from *B. cereus* in complex with GlcN(α1→6)Ins was solved by difference Fourier methods using the structure of the free enzyme (Heinz et al., 1995) as the model for phasing. Due to slight changes in cell dimensions, this initial difference Fourier map was relatively noisy with an *R*-factor of 33.6% (R_{free} = 36.5%) using the data above 1σ from 8 to 2.6 Å. The strongest positive electron density feature was found in the active site pocket of PI-PLC, showing very clear density for the *myo*-inositol ring but weaker density for the glucosamine moiety of GlcN(α1→6)Ins. Rigid body and least squares refinement reduced the *R*-factor to 22% using data from 8 to 2.2 Å. A newly

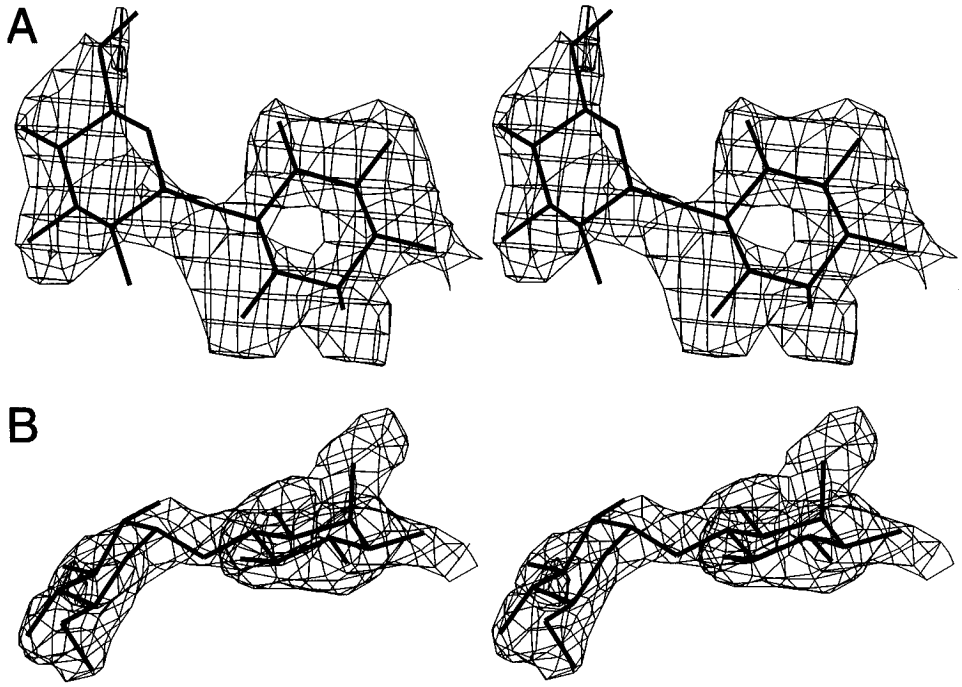

FIGURE 4: Stereo picture of a section of an initial $F_o - F_c$ difference Fourier map: (A) view looking down on the rings and (B) side view. The map shows electron density corresponding to the GlcN(α1→6)Ins molecule bound to the active site of *B. cereus* PI-PLC. The coefficients F_o and F_c are observed and calculated structure amplitudes, respectively, and α_c phases were calculated from the structure of the partially refined free enzyme, contoured at $+1.8\sigma$. Figures 4 and 5 were created using the program O (Jones et al., 1991).

calculated difference Fourier map (Figure 4) showed clearer density for GlcN(α1→6)Ins and a number of solvent molecules in the active site, most of which were present in the initial PI-PLC model and had been omitted prior to refinement. The remainder of the map was essentially featureless. At that point, GlcN(α1→6)Ins as well as most of the previously omitted solvent molecules were incorporated in the model and refinement was continued in combination with visual inspection of the model and gradual automatic incorporation of additional solvent molecules, for which the following criteria had to be passed for their inclusion in the model: positive density of $>3.5\sigma$ in the $F_o - F_c$ map, at least two hydrogen bonding partners present in the neighboring protein, and *B*-values of <50 Å^2 after final refinement. The final *R*-factor was 17.8% (R_{free} = 27.2%; Brünger, 1992) (Table 1). In the Ramachandran plot (Morris et al., 1992), 88.3% of the residues were in the most favored regions and only one residue (Asn189) was located in the disallowed region. This residue is located in a flexible surface loop (comprising residues 187−192) that is poorly defined in the electron density map. Weak electron density was also found for residues located in the loop comprising residues 237−243. The final model includes all residues except the C-terminal residues Lys297 and Glu298, for which essentially no electron density was found in the map.

Principal Features of the Structure of B. cereus PI-PLC. PI-PLC from *B. cereus* folds as an irregular TIM-barrel type $(\beta\alpha)_8$-barrel consisting of a central eight-stranded parallel β-barrel where the C-terminal end of one β-strand is linked to the N-terminal end of the next β-strand by an α-helical segment often in antiparallel orientation to the β-barrel (Farber, 1993). The PI-PLC structure is lacking two helices between strands IV and V and between V and VI, respectively (Figure 2; Heinz et al., 1995). Another feature departing from the canonical TIM-barrel is the presence of a β-strand (Vb) antiparallel to the other strands. Like in all other $(\beta\alpha)_8$-barrel-containing enzymes reported so far, the active site is located at the C-terminal side of the β-barrel. The active site pocket is oval-shaped, measuring approximately 15 × 9 Å in size and 12 Å in depth. The pocket is lined with a number of mainly charged amino acids that specifically interact with *myo*-inositol when complexed with PI-PLC (Heinz et al., 1995). It also contains the two histidines at positions 32 and 82, essential for catalysis (Heinz et al., 1995). The rim of the active site pocket consists of several loops and a short α-helix (residues 42−48) and encircles the cleft in a horseshoe-like manner with an opening at one end (Figure 2). Helix 42−48, loop 237−243, as well as parts of a long loop comprising residues 73−90 that "close" the rim opposite to this opening contain an unusually large number of hydrophobic amino acids exposed to solvent (Pro42, Ile43, Val46, Trp47, Pro84, Leu85, Ala241, Trp242, and Pro245) that might play a role in observed interfacial activation of PI-PLC, i.e. the increase of catalytic activity in the presence of micellar and vesicular substrates (Lewis et al., 1993; Volwerk et al., 1994). Both helix 42−48 and loop 237−243 are rather flexible in the structure and presumably adopt different orientations or conformations when the enzyme approaches the membrane. At the "open" side of the rim, the active site pocket is linked to a more shallow channel at the surface that measures approximately 15 Å in length and extends toward the area where the two α-helices of the TIM-barrel are missing. This channel is lined by mainly polar amino acids.

The structure of PI-PLC in complex with GlcN(α1→6)-Ins presented here was solved at a higher resolution (2.2 Å) than the previously reported PI-PLC structures both in free form and complexed with *myo*-inositol (2.6 Å) (Heinz et al., 1995). As expected, the increase in resolution resulted in a much better defined overall structure but did not resolve areas in the structure that were poorly defined in the previous structures, e.g. the C-terminal residues Lys297 and Glu298.

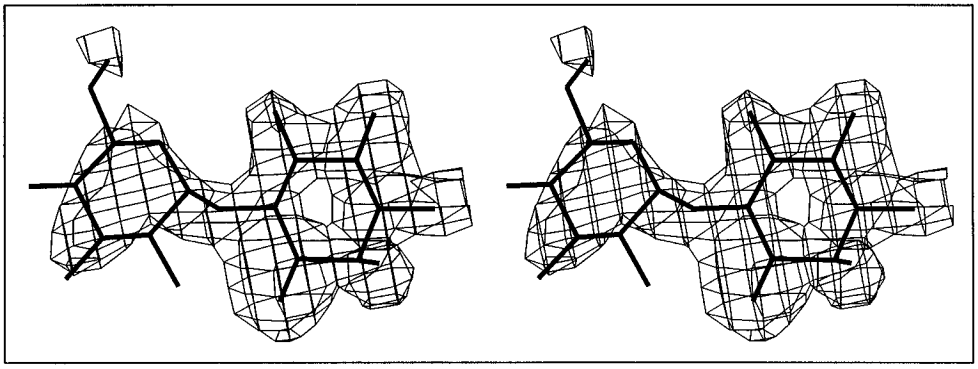

FIGURE 5: Stereo picture of the final ($2F_o - F_c$) electron density for GlcN(α1→6)Ins in the same orientation as in Figure 4A. The map was contoured at 1.2σ.

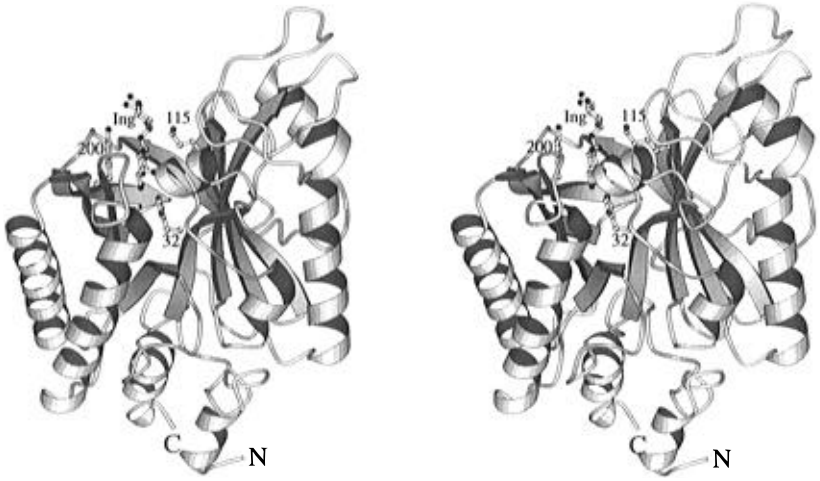

FIGURE 6: Stereo ribbon representation of *B. cereus* PI-PLC with GlcN(α1→6)Ins (labeled Ing) bound to the active site. The side chains of His32, Lys115, and Tyr200 are shown and labeled.

The rms deviation between the corresponding average main chain atom positions in free PI-PLC and the present complex was 0.31 Å. Larger rms deviations were found for residues belonging to flexible surface loops as well as the first five N-terminal residues.

Interactions of GlcN(α1→6)Ins with PI-PLC from B. cereus. The initial $F_o - F_c$ electron density map showed very clear density for the entire *myo*-inositol ring but considerably weaker density for parts of the glucosamine ring of GlcN(α1→6)Ins, suggesting increased flexibility or the presence of multiple conformations with respect to the *myo*-inositol moiety (Figure 4). Overall shape and the location of the density confirmed the chair conformation of the D-glucosamine and the α(1→6) glycosidic bond to the *myo*-inositol. Parts of the glucosamine ring still remain poorly defined or not defined in the final $2F_o - F_c$ map (Figure 5).

GlcN(α1→6)Ins binds to the center of the active site pocket via its *myo*-inositol moiety with the glucosamine pointing out of the active site toward solvent space (Figure 6). Therefore, most of the specific and close interactions with active site residues are made by the *myo*-inositol. When compared with the location of this moiety in the structure of the complex between PI-PLC and *myo*-inositol (Heinz et al., 1995), its position is virtually identical in the present structure. As in the former complex, specific hydrogen bonding interactions between the amino acids His32, Arg69, Arg163, and Asp198 of PI-PLC are formed with the hydroxyls OH2, OH3, OH4, and OH5 of *myo*-inositol (Figure 7 and Table 2). In addition, the ring stacks with its apolar face on top of the phenol ring of Tyr200. There are no solvent-mediated contacts between *B. cereus* PI-PLC and *myo*-inositol.

Table 2: Hydrogen Bonding Interactions between PI-PLC and GlcN(α1→6)Ins

atom in GlcN(α1→6)Ins	residue and atom in PI-PLC (distance in angstroms)
OH2	His32 $N^{\epsilon 2}$ (3.1), Arg69 $NH^{\xi 2}$ (2.9)
OH3	Asp198 $O^{\delta 1}$ (2.8)
OH4	Arg163 $N^{\xi 1}$ (3.2), Arg163 $N^{\xi 2}$ (3.0), Asp198 $O^{\delta 2}$ (2.6)
OH5	Arg163 $N^{\xi 2}$ (2.8)
O5′	Lys115 N^{ζ} (3.2)
OH4′	Glu6 $O^{\epsilon 2}$ (2.5)[a]
OH6′	Ser2 N (3.2)[a]

[a] Residue located in symmetry-related molecule (unit cell translation along *y*-axis).

In contrast, essentially no specific interactions are observed between the glucosamine part of GlcN(α1→6)Ins and PI-PLC. There is only one potential hydrogen bond between the side chain of Lys115 and the ring oxygen (atom O5′) of glucosamine. Furthermore, there are two hydrogen bonds formed with N-terminal amino acids of a neighboring symmetry-related PI-PLC molecule (Figure 8, Table 2). These interactions with the protein may be responsible for restricting the observed flexibility of the glucosamine to the point where most of it becomes defined in the electron density map, and the interaction between the glucosamine

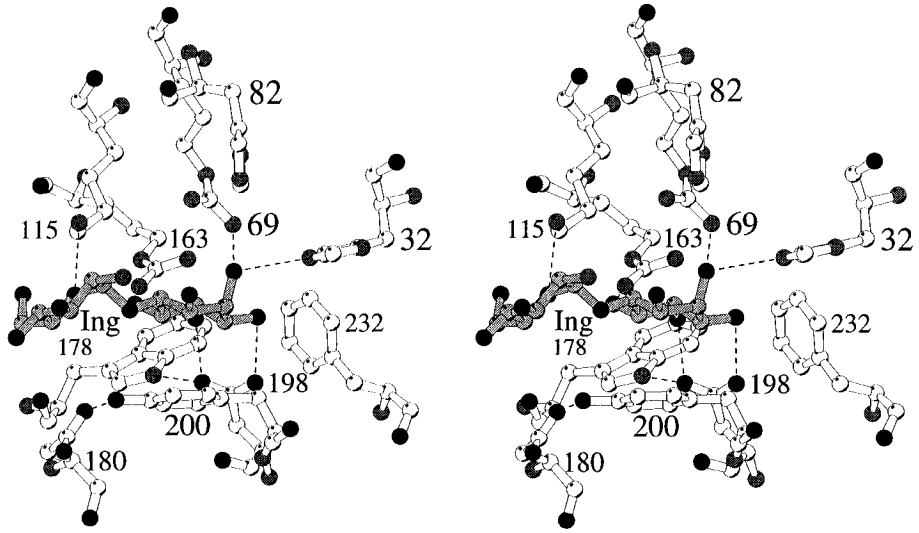

FIGURE 7: Stereo ball and stick representation of the interactions between GlcN(α1→6)Ins (side view, labeled Ing and shaded gray) and single amino acid residues in the active site of *B. cereus* PI-PLC. The PI-PLC residues shown and labeled are His32, Arg69, His82, Lys115, Arg163, Trp178, Asp180, Asp198, Tyr200, and Phe232. Hydrogen bonds are indicated by dotted lines. Oxygen atoms are drawn in black and nitrogen atoms in gray.

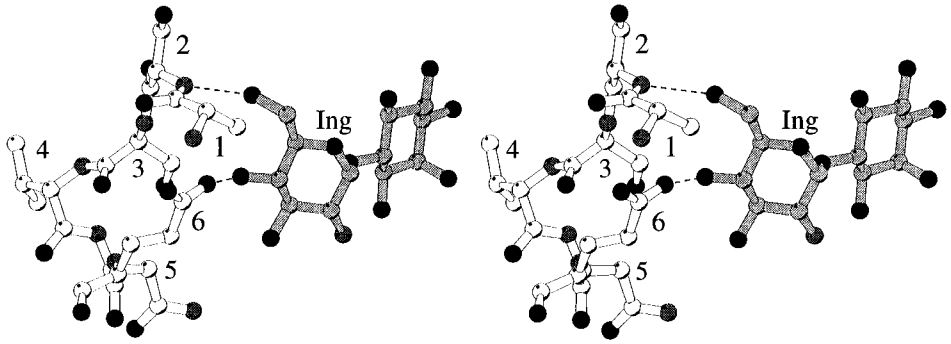

FIGURE 8: Stereo ball and stick representation of the interactions between GlcN(α1→6)Ins (labeled Ing and shaded gray) and N-terminal amino acids (1−6) of a symmetry-related neighboring *B. cereus* PI-PLC molecule. The PI-PLC residues shown are Ala1, Ser2, Ser3, Val4, Asn5, and Glu6. Hydrogen bonds are indicated by dotted lines. Oxygen atoms are drawn in black and nitrogen atoms in gray.

and PI-PLC may differ in the absence of this crystal contact. The crystals of the present complex grew larger and diffracted X-rays to a higher resolution (2.2 Å) than crystals previously obtained for free PI-PLC and in complex with *myo*-inositol (2.6 Å). It can, however, only be speculated whether this improvement is due to the slight increase of the number of interactions across this crystal contact or the presence of the inhibitor at the active site.

DISCUSSION

GPI anchors can be viewed as consisting of three parts: the lipid anchor, the *myo*-inositol 1-phosphate, and the oligosaccharide chain (Figure 1). The lipids of GPI anchors exhibit considerable diversity. A variety of saturated and unsaturated fatty acids are found in GPI anchors, and *B. cereus* PI-PLC cleaves these anchors (Roberts et al., 1987, 1988a). It has also been demonstrated that bacterial PI-PLCs are insensitive to the fatty acid composition of PI (Kume et al., 1992).

The hydrocarbon chains of GPI anchors are linked to glycerol by ester bonds (i.e. diacylglycerols) or by ether bonds (i.e. 1-alkyl-2-acyl glycerol), or the alkyl/acyl glycerol of the anchor can be replaced by ceramides. *B. cereus* PI-PLC cleaves all of these types of GPI anchors (Guther et al., 1994). The enzyme also displays a lack of stereospecificity toward the 1,2-DAG moiety of PI (Bruzik et al., 1992), suggesting that the enzyme does not specifically recognize this part of the molecule. This lack of specificity for the lipid component is consistent with the crystal structure of PI-PLC. In contrast to the deep active site pockets of phospholipases A_2, which show extensive interactions with fatty acids of the lipid substrate via a 14 Å deep hydrophobic channel extending from the catalytic site to the surface of the molecule (Scott et al., 1990), the active site pocket of *B. cereus* PI-PLC is less deep and mainly polar with a few hydrophobic amino acids located at the rim of the pocket that could potentially interact with the apolar part of a membrane (Figure 2). These amino acids are more likely to be important for interfacial activation observed for the enzyme.

The specific recognition of a GPI anchor by *B. cereus* PI-PLC is provided by the *myo*-inositol moiety. Of the nine possible stereoisomers of inositol, GPIs, like PIs, contain predominantly one isomer, *myo*-inositol. A minor proportion of GPIs contain *chiro*-inositol, but it is unknown whether these are substrates for any PI-PLCs or GPI-PLCs (Rademacher et al., 1994; Bruzik et al., 1994; Farese et al., 1994). *B. cereus* PI-PLC is stereospecific for PI-derived substrates containing the D-enantiomer of *myo*-inositol, and the L-enantiomer is neither a substrate nor an inhibitor (Volwerk et al., 1990; Leigh et al., 1992; Lewis et al., 1993; Bruzik et al., 1992; Bruzik & Tsai, 1994). It has been established by

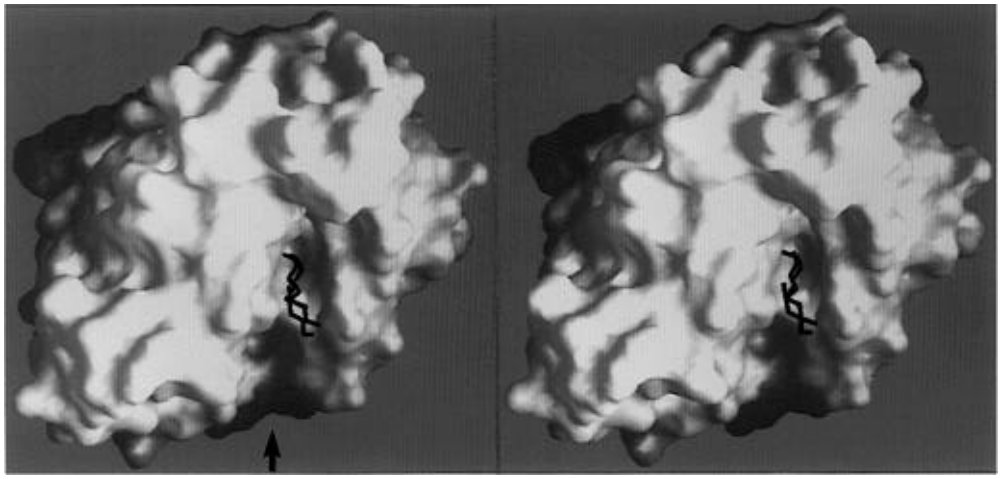

FIGURE 9: Stereo picture of a van der Waals surface representation of the C-terminal side of *B. cereus* PI-PLC, with GlcN(α1→6)Ins bound to the active site pocket near the center (molecule shown in black). The shallow polar channel which may accommodate one or two additional glycan residues of the GPI anchor is identified by an arrow. The picture was generated using the program GRASP (Nicholls, 1993).

NMR that *B. cereus* PI-PLC acts as a phosphotransferase, cleaving PI to form the water-soluble component, *myo*-inositol 1:2-cyclic phosphate [I(1:2cyc)P], and lipid-soluble DAG. Subsequently, in a much slower reaction, the enzyme acts as a phosphodiesterase, converting I(1:2cyc)P to *myo*-inositol 1-phosphate (Volwerk et al., 1990). The primary products of cleavage of GPI anchors by *B. cereus* PI-PLC are DAG and, evidently, the corresponding *myo*-inositol 1:2-cyclic phosphate (Jäger et al., 1990; Hooper et al., 1991). Structural and kinetic evidence indicate that the mechanism of cleavage of PI by *B. cereus* PI-PLC is an acid−base catalysis similar to that of ribonuclease A. In PI-PLC, His32 is in a position to act as a base, abstracting a proton from the axial 2-OH of the inositol ring, promoting nucleophilic attack by this axial 2-OH oxygen on phosphorus and simultaneous donation of a proton to the scissile bond by His82 which acts as the acid. This mechanism involves a pentacovalent transition state and inversion around phosphorus to form the I(1:2cyc)P product (Bruzik & Tsai, 1994; Volwerk et al., 1990). The importance of the axial 2-OH of *myo*-inositol in the catalytic mechanism is supported by the fact that GPI anchors which have the 2-OH esterified (e.g. palmitated) are resistant to cleavage by *B. cereus* PI-PLC (Roberts et al., 1988b). Likewise, synthetic derivatives of PI in which the 2-OH of *myo*-inositol is blocked or missing are not cleaved (Lewis et al., 1993). Thus, the cleavage of PI and GPI anchors by PI-PLC is very similar. This is entirely consistent with the structural data presented here. The crystal structures of PI-PLC complexes reveal that *myo*-inositol alone and the *myo*-inositol moiety of GlcN(α1→6)-Ins occupy virtually identical locations in the active site of *B. cereus* PI-PLC, confirming that the enzyme utilizes the same catalytic mechanism for cleavage of PI and GPI anchors. This must also be true for *B. thuringiensis* PI-PLC, since the two enzymes differ by only eight amino acids that are not involved in catalysis or substrate binding. Structurally significant sequence similarities with other bacterial PI-PLCs and some homology to the GPI-PLC of *T. brucei* have been noted previously (Heinz et al., 1995), suggesting that the mechanisms of GPI and PI cleavage are similar for these enzymes as well.

There are several enzyme kinetic studies which can be correlated with the crystal structure. *myo*-Inositol is a weak inhibitor of *B. cereus* PI-PLC, with an IC_{50} of 8 mM, measured with PI as the substrate solubilized in the detergent deoxycholate (Shashidhar et al., 1990). In a study aimed at determining the glycan requirements of *T. brucei* GPI-PLC, the inhibition of a series of small glycoinositol analogs of GPI, including GlcN(α1→6)Ins, was examined using the substrate VSG in deoxycholate micelles (Morris et al., 1995). An interesting aspect of this work is that it includes data on the cleavage of VSG by *B. cereus* PI-PLC as well as *T. brucei* GPI-PLC. GlcN(α1→6)Ins was found to be a weak inhibitor (28.9% inhibition at 5 mM) of *T. brucei* GPI-PLC, whereas under similar conditions, no inhibition of *B. cereus* PI-PLC was observed. Recently, the IC_{50} values of *myo*-inositol and GlcN(α1→6)Ins were found to be 9 and 2 mM, respectively, in a detergent-free assay of *B. cereus* PI-PLC utilizing the water-soluble substrate analog 4-nitrophenyl-*myo*-inositol 1-phosphate (M. Ryan, unpublished experiments). These three inhibition studies present a consistent picture, allowing for variations due to differences in assay conditions. The general observation is that both *myo*-inositol and GlcN(α1→6)Ins are weak inhibitors but sufficiently strong to displace solvent from the active site and produce the obtained complexes with PI-PLC. GlcN(α1→6)Ins is a slightly better inhibitor than *myo*-inositol, indicating limited rather than extensive additional interactions with residues in the active site region. This is consistent with the weak interaction we observe between the glucosamine moiety and *B. cereus* PI-PLC in the present crystal structure.

The glucosamine moiety of GlcN(α1→6)Ins protrudes away from the catalytic groups toward solvent. Because of its relative orientation, the glucosamine is not expected to interfere with the binding of the phospholipid part of the GPI; also, the glucosamine is at a greater than 10 Å distance from the active site rim that presumably interacts with the lipid part of GPI. A surface representation of *B. cereus* PI-PLC is presented in Figure 9, showing the positions of the *myo*-inositol and glucosaminyl groups of the inhibitor GlcN-(α1→6)Ins in the active site. The shallow polar channel at the surface which could accommodate the proximal region of the oligosaccharide GPI anchor is also identified. This channel extends from the opening in the rim that encircles the active site pocket.

The glucosamine moiety exhibits considerable conformational flexibility as expressed in a weaker electron density. Its location relative to the inositol is, however, unambiguous and favors the energy-minimized conformation where the amino group of the glucosamine comes relatively close to the 1-OH group of the inositol (Figures 4 and 5). Therefore, modifications of the amino group would be expected to interfere with the phosphate group attached to position 1 of the inositol in GPI. Modeling a phosphate group at this position indicates that there would be steric conflicts with any modification of the glucosamine amino group. This agrees well with the observation that the amino group of the glucosamine in GPI anchors is free in contrast to most other biological glycoconjugates (Englund, 1993). Furthermore, it has been observed that N-methylation of glucosamine in a GPI anchor reduces its sensitivity to *B. cereus* PI-PLC cleavage compared to that of the nonmethylated form (Jäger et al., 1990).

Kinetic data show that PI-PLC cleaves both PI and GPI anchors at comparable rates. However, two compensating effects are observed; the enzyme binds GPI-anchored proteins with a higher affinity than PI, but the turnover for GPI cleavage is slower. As a net result, the ratio V_{max}/K_M is approximately the same for the two substrates (Stieger & Brodbeck, 1991). These data can be interpreted to indicate that recognizes PI-PLC not only the PI moiety of the anchor but also some of the remaining components. In this case, the most likely place on the surface of PI-PLC for glycan recognition is the shallow channel extending from the active site pocket that contains a number of polar amino acids capable of forming hydrogen bonds with sugar molecules. Stieger and Brodbeck (1991) also report slight differences in K_M for PI-PLC with respect to different anchors, which seem to be due to the glycan composition of the respective anchor. However, highly specific interactions with the glycans seem unlikely as they often carry a wide variety of additional modifications, especially at the mannose ring adjacent to the glucosamine ring (Englund, 1993).

CONCLUSIONS

The crystal structure of *B. cereus* PI-PLC complexed with GlcN(α1→6)Ins, a central fragment of GPI anchors, provides higher-resolution structural data on the binding of *myo*-inositol and insights into how GPI anchors are cleaved by this enzyme. A comparison with the previously determined structure of the enzyme in complex with *myo*-inositol establishes that the inositol rings are in the same position, indicating that the mechanism of cleavage of GPI anchors is similar to that of the cleavage of PI. Whereas the *myo*-inositol lies within an active site pocket with many well-defined hydrogen bonding contacts with the enzyme, the glucosamine residue is less rigidly held. There is little space for structural modifications of the amine group of glucosamine, which provides an explanation for why GPI anchors are unmodified at this position. The crystal structure suggests that the remainder of the GPI-glycan is well outside the active site region, and additional contacts must exist only on the surface of the enzyme, making it possible for *B. cereus* PI-PLC to bind and cleave structurally diverse glycans. Given the fact that the sequences of *B. thuringiensis* and *B. cereus* PI-PLCs are nearly identical, the structural insights presented here apply to both enzymes.

ACKNOWLEDGMENT

We thank professors Brian W. Matthews and Georg Schulz for generously making their facilities available. We are also grateful to Dr. Ulrich Baumann for critical reading of the manuscript.

REFERENCES

Anderson, R. G. W., Kamen, B. A., Rothberg, K. G., & Lacey, S. W. (1992) *Science 255*, 410−411.
Brünger, A. T. (1992) *Nature 355*, 472−475.
Brünger, A. T., Karplus, M., & Petsko, G. A. (1989) *Acta Crystallogr. A45*, 50−61.
Bruzik, K. S., & Tsai, M.-D. (1994) *Bioorg. Med. Chem. 2*, 49−72.
Bruzik, K. S., Morocho, A. M., Jhon, D.-Y., Rhee, S. G., & Tsai, M.-D. (1992) *Biochemistry 31*, 5183−5193.
Bruzik, K. S., Hakeem, A. A., & Tsai, M.-D. (1994) *Biochemistry 33*, 8367−8374.
Bullock, T. L., Ryan, M., Kim, S. L., Remington, S. J., & Griffith, O. H. (1993) *Biophys. J. 64*, 784−791.
Engh, R. A., & Huber, R. (1991) *Acta Crystallogr. A47*, 392−400.
Englund, P. T. (1993) *Annu. Rev. Biochem. 62*, 121−138.
Farber, G. K. (1993) *Curr. Opin. Struct. Biol. 3*, 409−412.
Farese, R. V., Standaert, M. L., Yamada, K., Huang, L. C., Zhang, C., Cooper, D. R., Wang, Z., Yang, Y., Suzuki, S., Toyota, T., & Larner, J. (1994) *Proc. Natl. Acad. Sci. U.S.A. 91*, 11040−11044.
Ferguson, M. A. J., & Williams, A. F. (1988) *Annu. Rev. Biochem. 57*, 285−320.
Ferguson, M. A. J., Low, M. G., & Cross, G. A. M. (1985) *J. Biol. Chem. 260*, 14547−14555.
Ferguson, M. A. J., Homans, S. W., Dwek, R. A., & Rademacher, T. W. (1988) *Science 239*, 753−759.
Guther, M. L. S., Cardoso de Almeida, M. L., Rosenberry, T. L., & Ferguson, M. A. J. (1994) *Anal. Biochem. 219*, 249−255.
Hamlin, R. (1985) *Methods Enzymol. 114*, 416−452.
Han, M. K., Yim, C.-Y., An, N.-H., Kim, H.-R., & Kim, U.-H. (1994) *J. Leukocyte Biol. 56*, 792−796.
Hawn, T. R., & Strand, M. (1993) *Mol. Biochem. Parasitol. 59*, 73−81.
Heinz, D. W., Ryan, M., Bullock, T. L., & Griffith, O. H. (1995) *EMBO J. 14*, 3855−3863.
Heise, N., Travassos, L. R., & Cardoso de Almeida, M. L. (1995) *Exp. Mycol. 19*, 111−119.
Hooper, N. M., Broomfield, S. J., & Turner, A. J. (1991) *Biochem. J. 273*, 301−306.
Howard, A. J., Nielsen, C., & Xuong, N. H. (1985) *Methods Enzymol. 114*, 452−472.
Jäger, K., Meyer, P., Stieger, S., & Brodbeck, U. (1990) *Biochim. Biophys. Acta 1039*, 367−373.
Jones, T. A., Zhou, J.-Y., Cowan, S., & Kjeldgaard, M. (1991) *Acta Crystallogr. A74*, 110−119.
Koke, J. A., Yang, M., Henner, D. J., Volwerk, J. J., & Griffith, O. H. (1991) *Protein Expression Purif. 2*, 51−58.
Kraulis, P. J. (1991) *J. Appl. Crystallogr. 24*, 946−950.
Kume, T., Taguchi, R., Tomita, M., Tokuyama, S., Morizawa, K., Nakachi, O., Hirano, J., & Ikezawa, H. (1992) *Chem. Pharm. Bull. 40*, 2133−2137.
Leigh, A. J., Volwerk, J. J., Griffith, O. H., & Keana, J. F. W. (1992) *Biochemistry 31*, 8978−8983.
Lewis, K. A., Garigapati, V. R., Zhou, C., & Roberts, M. F. (1993) *Biochemistry 32*, 8836−8841.
Lisanti, M. P., Rodriguez-Boulan, E., & Saltiel, A. R. (1990) *J. Membr. Biol. 117*, 1−10.
Low, M. G. (1989) *Biochim. Biophys. Acta 988*, 427−454.
Low, M. G., & Saltiel, A. R. (1988) *Science 239*, 268−275.
Meyer, J. E. W. (1996) Ph.D. Thesis, University of Freiburg, Freiburg, Germany.
Morris, A. L., MacArthur, M. W., & Thornton, J. N. (1992) *Proteins: Struct., Funct., Genet. 12*, 345−364.
Morris, J. C., Ping-Sheng, L., Shen, T.-S., & Mensa-Wilmot, K. (1995) *J. Biol. Chem. 270*, 2517−2524.

Müller, G., Gross, E., Wied, S., & Bandlow, W. (1996) *Mol. Cell. Biol. 16*, 442−456.
Nicholls, A. J. (1993) *GRASP Manual*, Columbia University, New York.
Plourde, R., d'Alarcao, M., & Saltiel, A. R. (1992) *J. Org. Chem. 57*, 2606−2610.
Rademacher, T. W., Caro, H., Kunjara, S., Wang, D. Y., Greenbaum, A. L., & McLean, P. (1994) *Braz. J. Med. Biol. Res. 27*, 327−341.
Roberts, W. L., Kim, B. H., & Rosenberry, T. L. (1987) *Proc. Natl. Acad. Sci. U.S.A. 84*, 7817−7821.
Roberts, W. L., Myher, J. J., Kuksis, A., Low, M. G., & Rosenberry, T. L. (1988a) *J. Biol. Chem. 263*, 18766−18775.
Roberts, W. L., Santikarn, S., Reinhold, V. N., & Rosenberry, T. L. (1988b) *J. Biol. Chem. 263*, 18776−18784.
Rosenberry, T. L., Toutant, J.-P., Haas, R., & Roberts, W. L. (1989) *Methods Cell Biol. 32*, 231−255.
Scott, D. L., White, S. P., Otwinowski, Z., Yuan, W., Gelb, M. H., & Sigler, P. B. (1990) *Science 250*, 1541−1546.
Shashidhar, M. S., Volwerk, J. J., Keana, J. F. W., & Griffith, O. H. (1990) *Biochim. Biophys. Acta 1042*, 410−412.
Stieger, S., & Brodbeck, U. (1991) *Biochimie 73*, 1179−1186.
Takeda, J., & Kinoshita, T. (1995) *Trends Biochem. Sci. 20*, 367−371.
Turner, A. J., Ed. (1990) *Molecular and Cell Biology of Membrane Proteins. Glycolipid Anchors of Cell-surface Proteins*, pp 5−220, Ellis Horwood Ltd., Chichester, West Sussex, U.K.
Vogel, M., Kowalewski, H., Zimmermann, H., Hooper, N. M., & Turner, A. J. (1992) *Biochem. J. 284*, 621−624.
Volwerk, J. J., Shashidhar, M. S., Kuppe, A., & Griffith, O. H. (1990) *Biochemistry 29*, 8056−8062.
Volwerk, J. J., Filthuth, E., Griffith, O. H., & Jain, M. K. (1994) *Biochemistry 33*, 3464−3474.
Vriend, G., & Sander, C. (1993) *J. Appl. Crystallogr. 26*, 47−60.

BI9606105